

NILU: TR 01/2005
REFERENCE: N-104007
DATE: DECEMBER 2005
ISBN: 82-425-1670-7

**Investigation of mercury
depletion events recorded
during early and late spring
2003 at Zeppelin / Ny-Ålesund,
Svalbard, Norway**

Lucas Girard, Torunn Berg and Lars R. Hole

NILU: TR 01/2005
REFERENCE: N-104007
DATE: OCTOBER 2005
ISBN: 82-425-1670-7

Investigation of mercury depletion events recorded during early and late spring 2003 at Zeppelin / Ny-Ålesund, Svalbard, Norway

Lucas Girard¹⁾, Torunn Berg²⁾ and Lars R. Hole²⁾

- 1) Lucas Girard – Master student at the University Centre on Svalbard (UNIS), the Norwegian Institute for Air Research (NILU) and the University of Technology of Belfort-Montbéliard (UTBM) (lucas.girard@utbm.fr)
- 2) Torunn Berg (NILU, tbe@nilu.no)
- 2) Lars R. Hole (UNIS/NILU, lrh@nilu.no)

Contents

	Page
Summary	5
1 Introduction	7
1.1 Mercury in the environment.....	7
1.1.1 Sources of mercury.....	8
1.1.2 Bioaccumulation and high levels of mercury in the Arctic.....	9
1.2 Springtime depletion of atmospheric mercury	10
1.2.1 A large scale phenomenon occurring in polar areas.....	10
1.2.2 Tropospheric ozone depletion events	10
1.2.3 Hypothetical chemistry of AMDEs	11
1.3 Implication of the depletion events in the cycle of mercury	11
1.3.1 Fate of the products	11
1.3.2 Local reactions and transported events	12
2 Instruments and methods	12
2.1 Sampling location.....	12
2.2 Local meteorology at the Zeppelin station.....	13
2.3 Monitoring of gaseous elemental mercury.....	14
2.4 Ozone monitoring.....	14
2.5 Atmospheric particles monitoring.....	14
2.6 Bromine maps and backward trajectory calculations.....	15
2.7 Definition of an AMDE	15
3 Results	15
3.1 Time series of GEM, ozone and meteorological data	15
3.2 Mean concentration of GEM and variations during the rest of the year	18
3.3 Atmospheric particles evolution during AMDEs.....	19
4 Discussion.....	19
4.1 Connections between AMDEs and local meteorology	19
4.1.1 Temperature.....	19
4.1.2 Shifting weather conditions.....	20
4.2 Characterisation of AMDEs using global weather data.....	21
4.2.1 Investigating the nature of AMDEs.....	21
4.2.2 AMDE 1, 31 March – 01 April	21
4.2.3 AMDE 2, 08-10 April	22
4.2.4 AMDE 3, 15-17 May.....	22
4.3 Atmospheric particles evolution	23
5 Conclusions	23
6 Acknowledgements.....	23
7 References	24
Appendix A AMDE 1: 31st March / 1st April	29
Appendix B AMDE 2: 8th-10th April.....	33
Appendix C AMDE 3: 15th-17th May	37

Summary

Since February 2000, gaseous elemental mercury (GEM) is continuously monitored at the Zeppelin station, close to Ny-Ålesund. The concentration of GEM remains quite constant throughout the year, around the background value, except for a three month period following the polar sunrise during which it encounters several rapid depletions, dropping down to very low levels, below the detection limit. These events are referred to as atmospheric mercury depletion events (AMDEs) and they are likely to be the result of the oxidation of GEM by bromine (BrO) free radicals. Using the Zeppelin station data, two different periods were studied for AMDEs in early and late spring 2003 ((a)17/03 to 14/04 and (b)04/05 to 30/05). The period in between, during which a field campaign took place, was already intensively studied for AMDEs (Gauchard *et al.*, 2005).

Three AMDEs were observed and investigated in the studied periods (a) and (b). Using local and global weather data, BrO maps, backward trajectories and calculated decrease rate of GEM, the origin of these events was researched. The two events of early spring appeared to be the result of more local chemistry (less than a day of travel time to Ny-Ålesund) than the event of late spring. Possible locations of the reactions causing this late event extend on an area between northwest Greenland and around Ellesmere Island. As expected these results follow the same pattern as the “bromine explosion” (sudden increases in BrO), starting at lower latitudes (i.e. 78°N) in March and moving poleward with the sun rising there.

Investigation of mercury depletion events recorded during early and late spring 2003 at Zeppelin / Ny-Ålesund, Svalbard, Norway

1 Introduction

1.1 Mercury in the environment

Sometimes referred to as one of the most interesting elements, Mercury has numerous physical and chemical properties. The other name of mercury, ‘quick-silver’, describes very well its most astonishing property, it is the only metal liquid at room temperature (Schroeder and Munthe, 1998).

Mercury was well known by the ancients and has been used through ages mainly for its ability to dissolve gold and silver. Nevertheless, it is nowadays mostly known for its extreme and pronounced toxicity, an aspect that was tragically demonstrated by several episodes of environmental contamination due to increased industrial use during the last century, sometimes leading to human poisoning (Poissant *et al.*, 2002).

One of the earliest example of mercury poisoning occurred in Japan in 1953, at Minamata. Ingestion of fishes contaminated by mercury discharged from a chemical manufacturer plant provoked an unknown disease, later referred to as the “Minamata disease” (Imura *et al.*, 1971). Four decades later more than 1200 people have died with the disease and a similar number were certified as having the Minamata disease (Takizava and Osame, 2001).

However, mercury is ubiquitous, being found in all environmental compartments (Poissant *et al.*, 2002) in rather low concentrations. It is emitted into the atmosphere from anthropogenic (i.e. combustion of coal, dental fillings) and natural (i.e. volcanic eruptions) sources (Ebinghaus *et al.*, 1999).

Mercury is found in the atmosphere as gaseous elemental mercury (GEM or Hg⁰) and mercury compounds such as particulate mercury (mercury associated to particles). However, the atmospheric residence time of mercury compounds and particulate mercury is relatively short, therefore these species will mostly be found near their sources and will deposit quickly. The rather long atmospheric residence time of GEM, around one year (Lindqvist and Rodhe, 1985; Slemr *et al.*, 1985), makes it the main specie of mercury found in the atmosphere.

GEM undergoes long-range transport over the globe and has therefore a globally uniform distribution (Bergan *et al.*, 1999), meaning that more or less the same background concentration can be expected for GEM at any place on the globe not close to a source.

As shown in Table 1, in the northern Hemisphere, the mean concentration of GEM varies between 1.4 and 1.7ng/m³ in remote areas. Inside cities much greater values can be expected because of nearby sources. The low value for Antarctica

confirms the importance of anthropogenic emissions; furthermore most of the emissions of mercury to the atmosphere occur in the northern hemisphere (AMAP, 1998).

Table 1: Annual mean concentrations of Hg⁰ at different locations.

Location	Mean concentration of Hg ⁰ (ng/m ³)		Source
	min	max	
Zeppelin, Svalbard (2000-2002)	1.47	1.59	Berg and Aspmo, 2003
Alert, Canada (1995-1999)	1.54	1.60	Schroeder <i>et al.</i> , 1998
Station Nord, Greenland (2002)	1.37	1.61	Dommergue <i>et al.</i> , 2003
Québec, Canada (1998)	1.62	1.79	Poissant, 2000
Germany / Sweden (1995)	1.53	1.93	Schmolke <i>et al.</i> , 1999
Seoul, Korea (1990s)	1.42	9.26	Kim and Kim, 2001
Antarctica	1.04		Ebinghaus <i>et al.</i> , 2002

1.1.1 Sources of mercury

Natural sources emit mercury mainly in the gaseous phase (Lindberg and Stratton, 1998). Mercury is released from the soils, the oceans, lakes, through volcanic and geothermal activity (Nriagu, 1989). Geologically Hg-enriched soils, located close to areas with intense tectonic activity are also an important natural source (Jonasson and Boyle, 1972).

Human activities have modified the natural cycle of mercury; emissions from oceans and soils probably include reemission of mercury from anthropogenic sources. It is therefore complex to evaluate the importance of natural emissions of mercury. The world flux of mercury from natural sources emitted to the atmosphere is in the order of magnitude of 2500 tons a year (Nriagu, 1989) with uncertainty of 100%.

Most of the anthropogenic emissions of mercury occur with combustion of a material containing mercury. Fossil fuel combustion (especially coal, secondly oil and wood) and waste incineration are the main sources (Pacyna and Pacyna, 2002).

As illustrated on Figure 1, anthropogenic emissions of mercury are about 2000 tons a year (Pacyna and Pacyna, 2002), with uncertainty of 30%. Hence, natural and anthropogenic fluxes of mercury to the atmosphere are in the same order of magnitude.

The considerable amount of mercury emitted through human activities since the late nineteenth century has modified the cycle of mercury and its concentrations in all environmental reservoirs. In the northern hemisphere, the average concentration of mercury is now about 1,8ng/m³, whereas it was probably around 0.5 ng/m³ in the nineteenth century (Ebinghaus *et al.*, 2002).

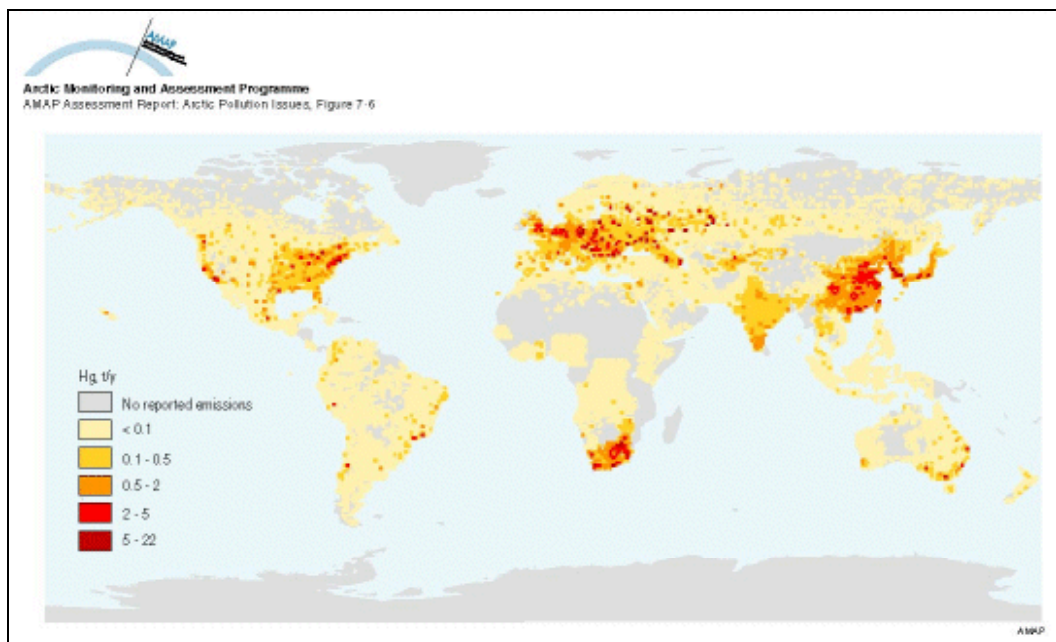


Figure 1: Spatial distribution of global emissions of Hg in 1990 within a $1^\circ \times 1^\circ$ grid. The total emission inventory is 2144 tonnes Hg. (AMAP, 1998).

1.1.2 Bioaccumulation and high levels of mercury in the Arctic

Mercury is one of the major pollutants in the Arctic environment, it is found at high levels in marine animals at many places in the Arctic and north Atlantic Ocean (AMAP, 2002).

In the water, divalent mercury is bioaccumulated in pelagic food chains and can be transformed into methyl-mercury (the most toxic mercury compound). Mercury biomagnifies along the food chains, meaning that bioaccumulation increases with trophic level. Survey data show that mercury concentration in marine animals is often correlated with body size (Watras *et al.*, 1998).

Local populations of the Arctic, e.g. Inuit, traditionally feed on other carnivores such as seals and small cetaceans (belugas and narwhals) that are at the top of the food chains. They are therefore exposed to the high concentrations of mercury bioaccumulated in these animals (Hansen, 2000).

The Arctic Monitoring and Assessment Programme (AMAP), created in 1991 in order to initiate a continuous monitoring of pollutants on a circumpolar scale and their effects on human health, has given evidence of increasing concentrations of mercury among the native human-beings of the Arctic.

The cause of the rise in mercury contamination in Arctic areas is still under discussion but one of the reasons could be a modification in the chemistry of the polar atmosphere (Gauchard *et al.*, 2005). Atmospheric mercury depletion events (AMDE), which will be described in the next chapter, could explain some of these modifications.

1.2 Springtime depletion of atmospheric mercury

1.2.1 A large scale phenomenon occurring in polar areas

In 1995, the first continuous measurements of atmospheric mercury in Polar Regions were realised at Alert, Canada (82North) revealing an unexpected phenomenon. During a three-month period following the polar sunrise, the concentration of GEM showed high variations, dropping to very low levels below the detection limit of the instrument (Schroeder *et al.*, 1998). It remained quite stable around the average value of $1.7\text{ng}/\text{m}^3$ for the rest of the year.

This discovery can be regarded as surprising since GEM otherwise exhibits an almost globally uniform distribution with an atmospheric lifetime of about one year (Schroeder and Munthe, 1998).

This phenomenon, referred to as atmospheric mercury depletion events (AMDEs), has since then been observed at several locations in the Arctic, the sub-Arctic and in the Antarctic as shown in Table 2. AMDEs are therefore occurring on a very large scale and it appears necessary to understand the chemistry responsible for this phenomenon to evaluate its consequences on the cycle of mercury.

Table 2: Observations of AMDEs in Polar Regions.

	Location	Reference
Arctic	Alert, Canada	Schroeder <i>et al.</i> , 1998
	Barrow, Alaska	Lindberg <i>et al.</i> , 2002
	Station Nord, Greenland	Skov <i>et al.</i> , 2004
	Ny-Ålesund, Svalbard	Berg <i>et al.</i> , 2003
	Amderma, Russia	Steffen <i>et al.</i> , 2004
	Flights measurements over sea ice, Canada	Banic <i>et al.</i> , 2003
Sub-Arctic	Kuujuarapik and Whapmagoostui, Quebec	Poissant <i>et al.</i> , 2002
Antarctic	Neumayer station	Ebinghaus <i>et al.</i> , 2002
		Temme <i>et al.</i> , 2003
	Terra Nova B	Sprovieri <i>et al.</i> , 2002

1.2.2 Tropospheric ozone depletion events

The first analyses of mercury depletion events showed a clear correlation with tropospheric ozone depletion events (ODE), a phenomenon first reported by Bottenheim *et al.* (1986) at Alert.

Following the same variation pattern as elemental mercury, tropospheric ozone is stable most of the year at its background concentration ($60\text{-}80\ \mu\text{gm}^{-3}$) except during the three months following the polar sunrise (March-May) during which it encounters several rapid depletions, down to very low concentrations (less than $4\ \mu\text{gm}^{-3}$).

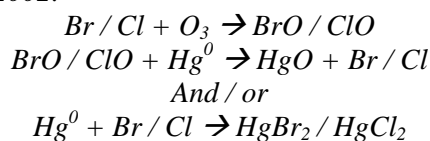
Various studies of ODEs propose reactions involving halogen atoms, especially bromine, to explain the phenomenon (e.g. Barrie *et al.*, 1988). Molecular halogens such as Br₂ and BrCl are emitted from aerosols, snow and frozen surfaces (Rankin *et al.*, 2002), which produce active bromine radicals Br through photolysis. These radicals destroy ozone to form BrO radicals. ODEs have also been observed in the stratosphere where chlorine, produced in the polar stratospheric clouds, could explain the phenomenon.

According to these hypotheses, the specific conditions occurring during the polar spring are necessary to start ODEs, including frozen surfaces (e.g. sea ice), therefore temperatures around -10/-20 degrees and sunlight to trigger the reactions.

1.2.3 Hypothetical chemistry of AMDEs

The main hypothesis explaining the chemistry of AMDEs is, as for ODEs, involving halogen chemistry and bromine in particular. Bromine free radicals (Br and BrO) react with elemental mercury to form oxidised species (Lindberg *et al.*, 2002). The product of these reactions is reactive gaseous mercury (RGM); a portion of it will form particulate mercury (Hg-P) by adsorption onto atmospheric particles.

After Lindberg *et al.*, 2002:



Contrary to ODEs, during which ozone is destructed, during AMDEs elemental mercury is oxidised into less volatile species, which will quickly deposit.

1.3 Implication of the depletion events in the cycle of mercury

1.3.1 Fate of the products

Mercury depletion events are producing oxidised species, RGM and Hg-P, which have a much shorter atmospheric residence time than GEM, they are less volatile and will therefore quickly deposit on frozen surfaces.

Flux chamber measurements have shown that a part of the deposited products will be re-emitted to the atmosphere shortly after the depletion event through photo-induced reduction processes (Sommar *et al.*, 2004). The importance of this re-emission can be discussed but it probably explains the high concentrations of GEM sometimes observed after the depletion events (>2ng/m³). However, AMDEs probably increase the mercury deposition flux in Polar Regions significantly.

When the snow melts, oxidised mercury species, which are more soluble in water than GEM, are released in the marine environment. Large areas are therefore potentially affected by high concentrations of mercury, which is likely to increase bioaccumulation at a time of the year when the biotas are preparing for peak summertime activity (Schroeder *et al.*, 1998).

Consequently, depletion events can potentially explain the high levels of mercury found in the Arctic environment especially among marine ecosystems and native populations.

1.3.2 Local reactions and transported events

Since mercury depletion events occur in the troposphere, one must keep in mind that the depletions are not taking place on a precise area, they are associated to the movements of air mass.

An air mass which has encountered an AMDE and has therefore low concentration of mercury is likely to be advected elsewhere, keeping its low level of GEM for a variable time lapse. Thus, the observation of a depletion event can be whether due to local chemistry or to the advection of an air mass that previously reacted (“transport chemistry”). It appears therefore interesting to characterise the depletion events, by estimating their origin, the areas where the reactions actually occurred.

Most of the research concerning AMDEs in Ny-Ålesund has been focused on the period during which the field campaign occurs, this campaign being planned to hit the main depletion events, the most significant in duration and amplitude. In 2003, the field campaign covered all of April and this period was studied for AMDEs and their characteristics (Gauchard *et al.*, 2005). In this study, two periods, before and after (March and May) the campaign, were studied.

Temperature plays a very important role in AMDEs and it is supported that temperature below -10 are necessary to trigger a depletion event (Lu *et al.*, 2001; Lindberg *et al.*, 2002). Consequently AMDEs recorded in Ny-Ålesund in May, where -10 is a typical minimal temperature, should result of transport chemistry, the local temperature being not cold enough to trigger the reactions. This fact will be verified and if necessary, the location of reaction will be estimated using backward trajectories.

2 Instruments and methods

2.1 Sampling location

Continuous measurements of gaseous elemental mercury have been carried out by the Norwegian institute for air research (NILU) at Ny-Ålesund, Svalbard ($78^{\circ}54'N$, $11^{\circ}53'E$) since February 2000.

Ny-Ålesund is a small international settlement completely dedicated to polar research. It is located on the western coast of Spitsbergen (Figure 2), the biggest island of Svalbard. The air sampling is realised at the NILU research station, located on the nearby Zeppelin Mountain at 475m above sea level, accessible by cable car. The station is located on a mountain ridge, with steep downhill to the north and south, and higher mountain peaks to the west and east (altitude 1000-1500 m). The mountain station was established in order to minimize the influence from local pollution during low-level measurements of air pollutants (Berg *et al.*, 2003). Shallow surface inversions are common in the Arctic, and measurements down at Ny-Ålesund might therefore occasionally be exposed to the small

anthropogenic emissions from the nearby settlement, trapped in the inversions layer. This contribution is thought to be negligible at the Zeppelin station (Solberg *et al.*, 1996).

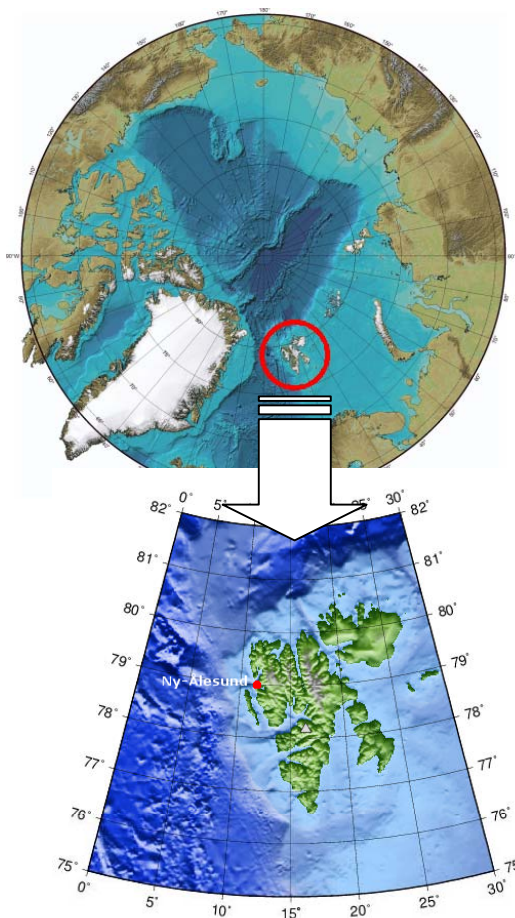


Figure 2: *The Arctic and Svalbard.*

2.2 Local meteorology at the Zeppelin station

In this study, local meteorological data (wind speed and direction, air temperature, air pressure, relative humidity) were used to characterise mercury depletion events. These data were recorded from the meteorological mast standing on the roof of the Zeppelin station.

It should be mentioned that local meteorology at the Zeppelin station is influenced by the topography of the area. Funnelling effects caused by the surrounding mountains, glaciers and valleys drive the wind direction (Beine *et al.*, 1996). Two specific directions are thus observed, south-easterly (prevailing) and north-westerly winds. Therefore, weather maps from GFS-Europe, available at Wetterzentrale (<http://www.wetterzentrale.de>) were also used to get a global overview of the meteorological conditions, sometimes mistaken in the local data.

2.3 Monitoring of gaseous elemental mercury

A Tekran Gas Phase Mercury Analyser (Model 2537A; Tekran Inc., Toronto, Canada) was installed at the Zeppelin station in February 2000 for measurements of GEM.

The pre-filtered sample air stream goes through gold cartridges where GEM is trapped. GEM is then thermally desorbed and detected by cold vapour atomic fluorescence spectrometry (CVAFS) ($\lambda=253.7$ nm) (Tekran, 1999). Dual gold cartridges allow alternate sampling and desorption, resulting in continuous measurement of GEM on a predefined time base. The detection limit of the instrument is below 0.1 ng/m^3 and the range of operation spans from 0.1 to 2000 ng/m^3 with an accuracy of 2% for concentrations below 200 ng/m^3 .

The sampling time was 30 min from the 1st February 2000, and decreased to 5 min from the 1st April 2000. A sampling flow rate of 1.5 l/min was used. The instrument was calibrated daily using an internal permeation source, verified by manual injections every 3 months. A heated sampling line was used to maintain constant temperature throughout the line. The line was mounted ≈ 3 m above the ground on a mast 2 m out of the roof at the Zeppelin station. To reduce the amount of water and/or particles entering the input line, a filter holder containing 2 mm Teflon filter (47 mm diameter) was mounted at the inlet of the sampling line. A recovery of 98% was normally obtained when checking the sampling line for recoveries and leaks (Berg *et al.*, 2003).

2.4 Ozone monitoring

As mentioned previously ODEs and AMDEs are closely related phenomena and they are usually monitored together. Thus, ozone data and correlation with GEM data were also investigated in this study.

A Model 400 ozone analyser from Advanced Pollution Instrumentation (USA) is installed at Zeppelin to monitor ozone. This instrument is based on UV spectrophotometry at 254 nm, with ozone concentrations following the Beer-Lambert law. The detection limit is around 6ppb ($12 \text{ } \mu\text{g/m}^3$) and the accuracy is 1 ppb.

2.5 Atmospheric particles monitoring

Correlation between variations of atmospheric particles (positive or negative depending on their size) has been observed during ODEs (Staebler *et al.*, 1994) and AMDEs (Gauchard *et al.*, 2004). At Zeppelin, a Differential Mobility Particle Sizer (DMPS) is used to monitor the variations of atmospheric particles with diameter between 0.02 and $0.7 \text{ } \mu\text{m}$, divided in 16 classes. The instrument measures the electrical mobility of particles, which is a measure of velocity of motion resulting from the force a particle experiences when placed in an electric field, and depends on particle size. Details of the calibration, performance and instrumental artefacts problems are given in Lundgren *et al.* (1979).

AMDEs resulting of local reaction are usually correlated with variations of small particles (e.g. 0.02 to $0.4 \text{ } \mu\text{m}$). Whereas AMDEs resulting of the advection of a

previously depleted air mass have proved to be anti-correlated with variations of big particles (e.g. $> 0.56 \mu\text{m}$) (Gauchard *et al.*, 2005). Such correlation / anti-correlation was researched among the AMDEs reported in this study.

2.6 Bromine maps and backward trajectory calculations

Daily GOME-BrO (Global Ozone Monitoring Experiment) maps, provided by the Institute of Environmental Physics in Bremen (<http://www.iup.physik.uni-bremen.de/gomenrt>), were used to localise the possible origin of the depletions, the areas with high enough concentration of bromine (BrO) to be able to oxidise elemental mercury. These maps were generated using DOAS algorithm on operational GOME level-1 data as described in Richter *et al.* (1998). It is important to mention that these maps give a BrO concentration integrated over the vertical column (troposphere and stratosphere), while AMDEs only occur in the troposphere. These data should therefore be used carefully.

Backward trajectories were calculated using the Hybrid single-particle Lagrangian integrated trajectory (HYSPLIT) model (Draxler and Rolph, 2003). The calculations were made interactively using the READY display system (Rolph, 2003), which is provided on the web by the Air Resources Laboratory, National Oceanic & Atmospheric Administration (<http://www.arl.noaa.gov/ready/hysplit4.html>).

The NCEP/NCAR Reanalysis meteorological dataset was used for the calculations. More information about this dataset can be found online (www.arl.noaa.gov/ready-bin/cdc.pl). The stability of the back trajectories was verified by expanding the starting area or by calculating at different ending heights.

2.7 Definition of an AMDE

AMDEs can be of different amplitudes and durations, lasting from a few hours to several days; however not all variations in GEM concentration during the spring are AMDEs. During an AMDE, the depletion of GEM is correlated with a depletion of tropospheric O_3 (ODE). We therefore propose the following definitions:

- A major AMDE consists of a decrease in GEM below $0.5\text{ng}/\text{m}^3$, correlated to a significant ODE.
- A minor AMDE consists of a decrease in GEM below $1\text{ng}/\text{m}^3$ also correlated to an ODE.

3 Results

3.1 Time series of GEM, ozone and meteorological data

Figure 3 and Figure 4 present the time series of ozone, GEM and local meteorological data during the early (17th March, 17th April 2003) and late spring (4-30 May 2003) respectively. From these figures four depletions events were identified (Table 3). The second depletion, which occurred around the 9th April,

has two distinct peaks (2a and 2b) separated by a high intermediate value (1.9 ng/m^3). These two peaks will be discussed individually.

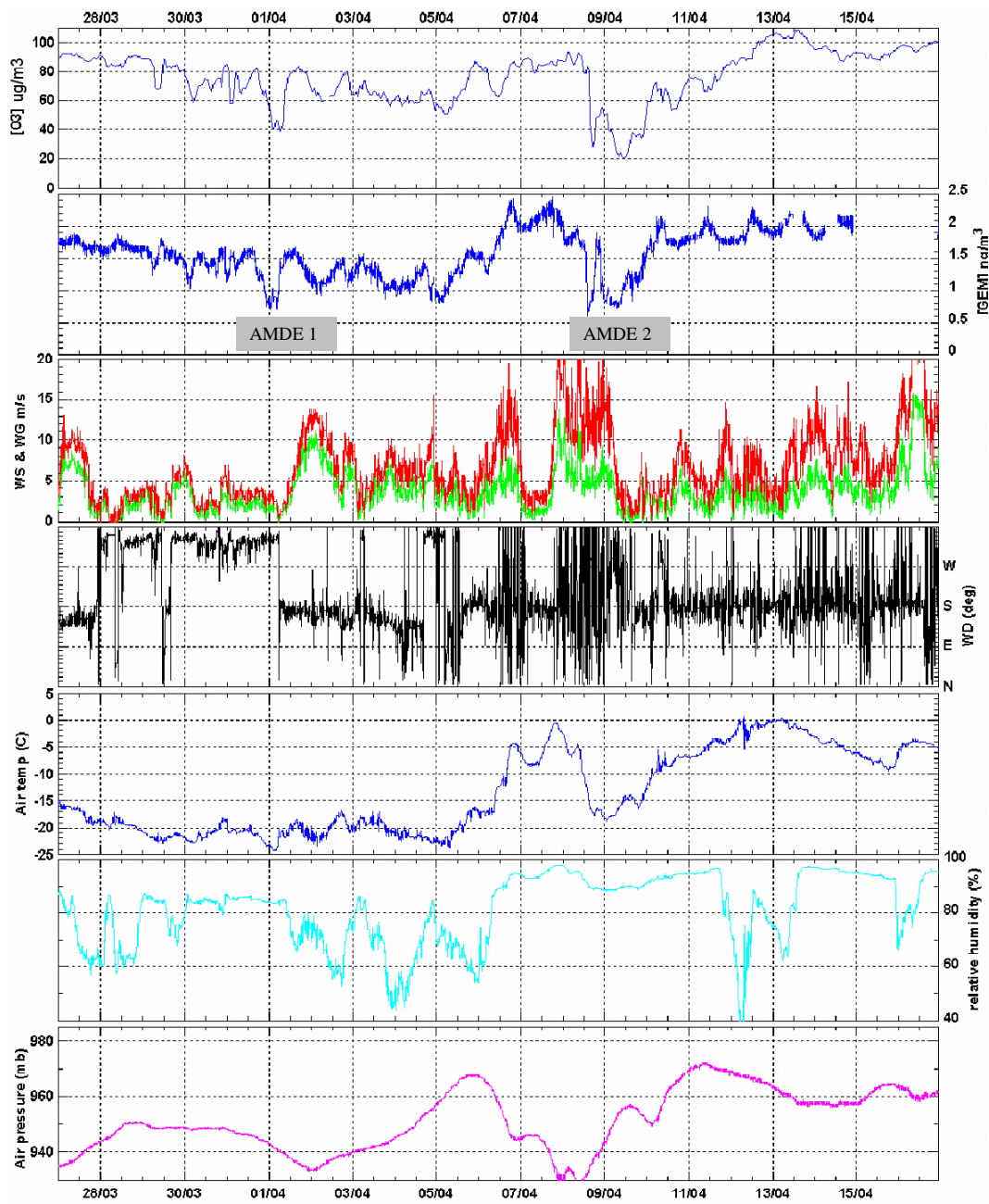


Figure 3: Early spring (27th March – 17th May 2003) time series of O_3 , GEM and local meteorology. Legend – WS: wind speed (green), WG: wind gust (red), WD: wind direction.

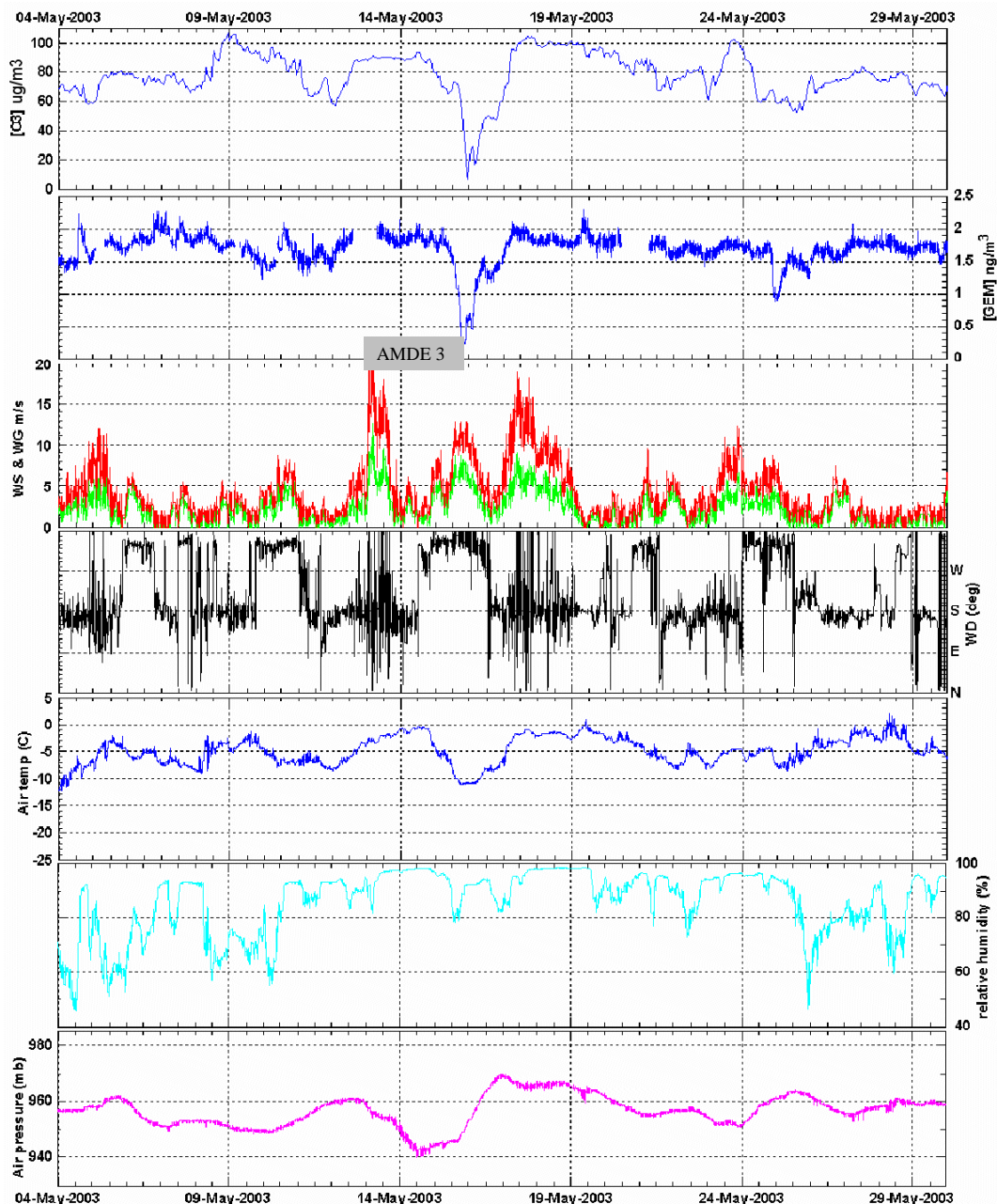


Figure 4: Late spring (4th May – 30th May 2003) time series of O₃, GEM and local meteorology. Legend – WS: wind speed (green), WG: wind gust (red), WD: wind direction.

ODEs were also identified and took place, as expected, simultaneously with the AMDEs, except for depletion 4 during which no significant variation of ozone is observed. Correlation coefficients for GEM and ozone were calculated during the depletion events (Figure 5).

According to the definitions proposed earlier, depletions 1 and 2 are minor AMDEs, depletion 3 is a major AMDE and depletion 4 is not an AMDE since it is not correlated to an ODE.

Table 3: AMDEs identified in the study period (2003).

Depletion		Date (GMT)	[GEM] in ng/m ³
1	Start	31-March 15:40	1.60
	Minimum	01-April 00:40	0.69
	End	01-April 08:05	1.45
2	Start	08-April 08:55	1.89
	Minimum	08-April 13:45	0.89
	Intermediate	08-April 19:25	1.91
	Minimum	09-April 07:05	0.71
	End	10-April 05:05	1.82
3	Start	15-May 09:25	1.80
	Minimum	15-May 19:15	0.14
	End	17-May 03:30	1.90
4	Start	24-May 19:55	1.65
	Minimum	24-May 23:10	0.84
	End	25-May 08:50	1.49

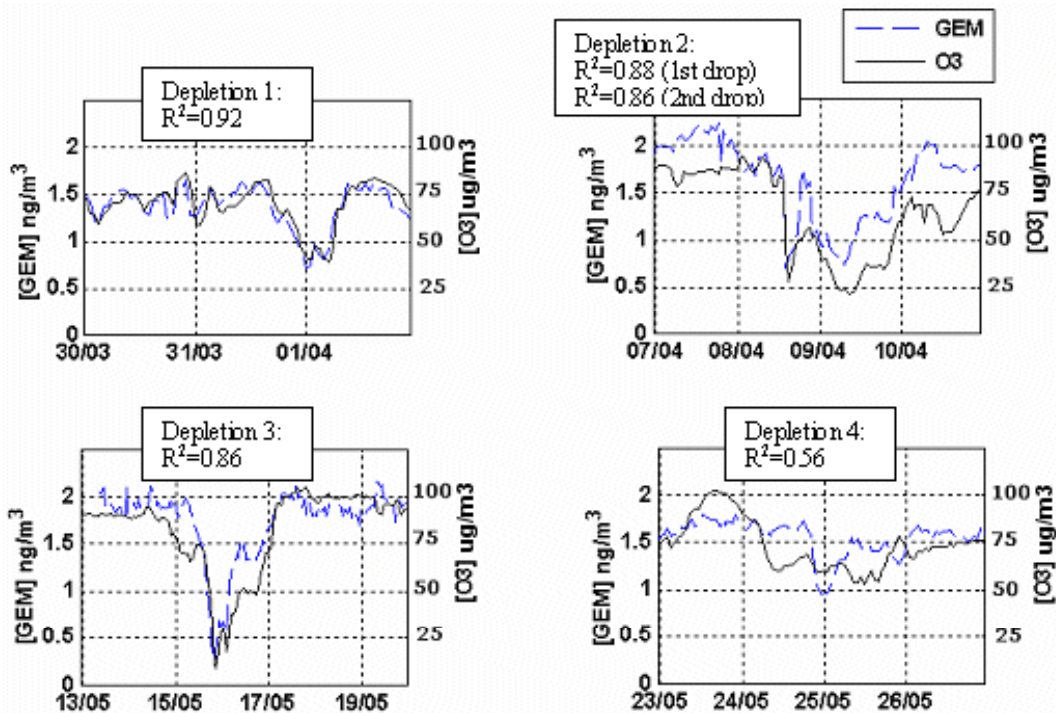


Figure 5: Correlation between ODEs and AMDEs.

3.2 Mean concentration of GEM and variations during the rest of the year

The annual mean concentration of GEM at Zeppelin is 1.60 ng/m³ for 2003. This result is in the same range as the previous observations reported in Berg and Aspö (2003), from 1.47 to 1.59 ng/m³ for 1995-2002. (Values for 1995-1999 being estimated from manual measurements.)

In total, 7 separate depletion events were observed in 2003, four major AMDEs occurred during the field campaign (17th April, 3rd May) and were investigated in

Gauchard *et al.* (2005). Finally 2 minor and one major AMDEs, took place in early and late spring and are reported in this study.

Concerning the rest of the year, small variations of GEM can be observed at the end of the winter in February, probably around the firsts apparitions of the sun, but GEM never drops below 1 ng/m³. On 11 June, a last minor event occurred, with GEM dropping down to 0.6 ng/m³, followed by very high values >2.5 ng/m³ on 14/06. During the summer and the autumn the concentration of GEM remains quite stable, with small fluctuations between 1.2 and 1.9 ng/m³.

3.3 Atmospheric particles evolution during AMDEs

Correlation between GEM and particles was researched for the three AMDEs, 10 different classes of particles were investigated. These classes can be grouped as in Gauchard *et al.* (2005) in small particles (17.8-56.2 nm) and big particles (>56.2 nm). Depletion 1 appears to be anti-correlated with variation of small particles, while depletion 2a shows anti-correlation with big particles. No clear trend was identified for depletion 2b and 3 (Table 4).

Table 4: Correlation coefficients (R^2) between concentration of GEM and atmospheric particles during the 4 AMDEs.

	Particle diameter	AMDE			
		1	2a	2b	3
"Small" particles	[17.8: 22.4] nm	-0.75	0.38	-0.49	-0.16
	[22.4: 28.2] nm	-0.75	0.44	-0.50	-0.15
	[28.2: 35.5] nm	-0.51	0.38	-0.39	-0.12
	[35.5: 44.7] nm	-0.44	0.26	-0.39	0.03
	[44.7: 56.2] nm	-0.20	-0.08	-0.38	0.13
"Big" particles	[56.2: 70.8] nm	-0.39	-0.35	-0.39	-0.03
	[70.8: 89.1] nm	-0.09	-0.64	-0.31	-0.30
	[89.1:112.2] nm	0.13	-0.69	-0.24	-0.41
	[112.2:141.3] nm	0.24	-0.70	-0.14	-0.42
	[141.3:177.8] nm	0.30	-0.73	0.01	-0.43

4 Discussion

4.1 Connections between AMDEs and local meteorology

By carefully studying the variations in local meteorology during AMDEs, a few suggestions can be established concerning the local / transport aspect of the depletion events.

4.1.1 Temperature

As mentioned earlier, temperature plays an important role in AMDEs (Lindberg *et al.*, 2002). Cold temperatures (below -10°C) are necessary to trigger a depletion event since they enable heterogeneous reactions of active bromine species onto frozen surfaces such as frost flowers or frozen sea-salt aerosols.

The AMDEs identified in the study period support that fact, being observed at air temperature between -25 and -10°C (Figure 6).

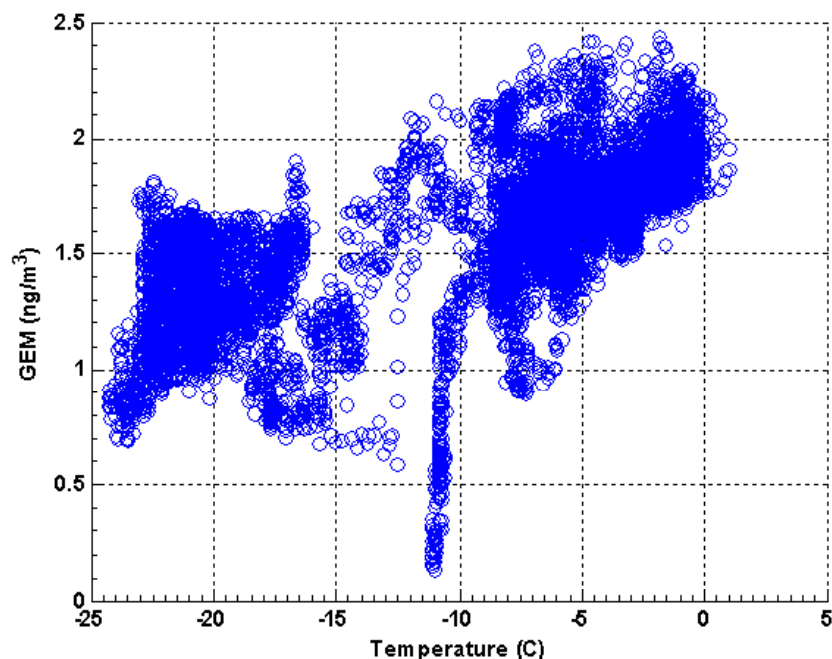


Figure 6: Scatter plot of GEM and temperature for the study period (17/03 to 14/04 and 04/05 to 30/05).

4.1.2 Shifting weather conditions

AMDE2 and AMDE3 occur in connection with major changes in the weather conditions. Between the 8th and 9th March the temperature drops from 0 to almost -20 and this drop is well correlated with the beginning of AMDE2. Although it is less clear, this change in weather is also seen in the wind (speed and direction).

A reason for this shift could be the presence of a low-pressure system on the North-East of Svalbard, associated with the passage of a cold front, leading to strong northerly wind. Such a shift in the weather creates important movements of air and it may have induced the advection of a depleted air mass to Ny-Ålesund, where it was recorded as AMDE2. This is supported by the fact that AMDE2 happens at the same moment as the weather shift. The same kind of scenario can be suggested for AMDE3.

Such depletion events are referred to as “transport events” in the literature (see 1.3.2). They occur when a depleted air mass is advected to the observation site after a day or more of travel time (>500km). In this way, AMDEs can be observed although no reactions are going on locally.

4.2 Characterisation of AMDEs using global weather data

Local meteorology gives hints about local / transport aspect of the studied AMDEs but a closer analyse is required to justify the nature of the events and to try to localise the origin of transport events. In order to do so, global weather data were used in connection with BrO maps.

4.2.1 Investigating the nature of AMDEs

The following parameters were considered together:

- BrO maps and 4 day backward trajectories ending in Ny-Ålesund
- GEM / O₃ rates of decrease
- Weather maps
- Without forgetting the first hints that were established using the local meteorology.

From the BrO maps, areas with high BrO concentrations were researched around Svalbard and along the backward trajectories to estimate the location of the reactions.

Tuckermann *et al.* (1997) compared O₃ rates of decrease ($\Delta O_3/\Delta t$), measured at a specific location during ODEs, to theoretical O₃ destruction rates obtained with a BrO/ClO mechanism. For these authors, rates of decrease around 4.5 ppb/h ($9 \mu\text{g m}^{-3}\text{h}^{-1}$) or more can only be attributed to advection of already depleted air masses.

O₃ and GEM rates of decrease ($\Delta \text{GEM}/\Delta t$) were calculated, together with relative rates of decrease (in order to compare O₃ to GEM):

$$\frac{\Delta \log c}{\Delta t} = \frac{\log(c(t_2)/c(t_1))}{t_2 - t_1}$$

Where $c(t)$ represents GEM or O₃ at time t .

These rates of decrease were compared to similar calculations made by Gauchard *et al.* (2005).

4.2.2 AMDE 1, 31 March – 01 April

During this first minor event (GEM dropping only to 0.7ng/m^3), the local meteorology shows rather stationary conditions with wind around 3m/s blowing from NW and temperature around -22°C . On 31/03 the BrO map shows quite high concentrations around Svalbard (Appendix A), thus this event could result of local chemistry. The decrease rates of GEM and O₃ are low (Table 5).

Backward trajectories show that the air mass has crossed the Arctic basin (Appendix A), from the Bering Strait. Unfortunately BrO maps in the end of March lack data in this area to attest that no other reactions happened before. Nevertheless, considering its modest importance, AMDE 1 is likely the result of local reactions.

Table 5: O_3 and GEM rates of decrease/increase for the 3 studied AMDEs.

AMDE		$\Delta O_3/\Delta t$ (ppb/h)	$\Delta \log(O_3)/\Delta t$	$\Delta GEM/\Delta t$ (ng/m ³ /h)	$\Delta \log(GEM)/\Delta t$
1	Decrease	-3.17	-0.06	-0.10	-0.09
	Increase	4.56	0.08	0.10	0.10
2	1st decrease	-10.42	-0.19	-0.27	-0.24
	1st increase	4.77	0.12	0.23	0.21
	2nd decrease	-2.92	-0.08	-0.10	-0.09
	2nd increase	2.87	0.07	0.05	0.04
3	Decrease	-6.58	-0.23	-0.16	-0.25
	Increase	2.61	0.07	0.05	0.08

4.2.3 AMDE 2, 08-10 April

This event exhibits two separate drops in GEM, a first one on the late 08/04 (AMDE 2a) and the other one on 09/04 (AMDE 2b).

Weather conditions were unsettled around Svalbard during this period, between the 8th and the 9th a low-pressure system passes from the West to the North-East of Svalbard, associated with strong winds. The temporary increase of GEM between AMDE 2a and 2b seem to happen at the same time as the shift in the weather.

High BrO concentrations in the Fram Strait area (between North-East Greenland and Svalbard) on the 8th could be responsible for a depletion (Appendix B), which could then be advected to Ny-Ålesund by the strong south-westerly winds and recorded as AMDE 2a. While AMDE 2b was probably caused by reactions around Franz Joseph archipelago, advected to Ny-Ålesund by easterly winds.

One could speculate whether the ‘BrO cloud’ located above Fram Strait on the 8th and the other one located above Franz Joseph archipelago on the 9th could be one, unique, cloud that would have been transported by the strong winds, which would link the origin of AMDE 2a and 2b. In order to answer this question, trajectories were calculated with HySplit (see paragraph 2.6), in forward mode, starting in Fram Strait (78.5N 10W) on the 8th. The resulting trajectory arrives 30hours later around Franz Joseph Islands. Consequently, the same ‘BrO cloud’ probably caused AMDE 2a and 2b.

AMDE 2 seems to be the result of reactions around the area of Svalbard and only involves short-range transport, a day or less of travel time.

4.2.4 AMDE 3, 15-17 May

On the 15th and 16th of May, a low-pressure system was building up on the north east of Svalbard, bringing cold air from northwest, leading to an considerable temperature drop (Figure 4). Backtrajectories indicates two possible origins (Appendix C), Fram Strait area for particles arriving at Ny-Ålesund on the late 15th and Ellesmere Island trough northern Greenland for particles arriving on the 16th.

The shifting weather conditions and fact that no high concentration of BrO was around Svalbard at this moment implies that AMDE 3 probably results of transport chemistry.

On the 12th, around Ellesmere Island, an area with significant concentration of BrO is crossed by the air mass that will arrive four days later in Ny-Ålesund. This hypothesis gives a possible explanation for AMDE 3 but is surprising considering that the depleted air mass would have been transported over 2000 km and still show a very low concentration of GEM in Ny-Ålesund.

4.3 Atmospheric particles evolution

No clear connection was identified between GEM and atmospheric particles. Considering the fact that the AMDEs investigated in this study are minor events and mostly result of transport chemistry, this result is not too surprising. Parallel evolution of atmospheric particles and GEM has mostly been observed for local AMDEs, on major events (Gauchard, personal communication).

5 Conclusions

During the period studied, early (17/03 to 14/04) and late (04/05 to 30/05) spring 2003, three AMDEs were observed and investigated. The two events of early spring turned out to be the result of more local chemistry than the event of late spring. The transport event of late spring was advected to Ny-Ålesund after reacting in areas further north (ca. 80-82°N).

The polar sunrise is the trigger for the “bromine explosions”, sudden increases in BrO due to heterogeneous reactions on highly saline surfaces. Areas with ‘clouds’ of high BrO column will be observed first at lower latitudes in March and later these areas are travelling poleward with the sun rising there (J. Hollwedel *et al.*, 2003). As a consequence AMDEs can be expected to follow the same pattern and it is therefore not surprising that among the 3 events investigated, the 2 events of early spring seem to have occurred further south (78-79°N) than the event of late spring.

Use of backward trajectories and BrO map has proved to be an interesting method to give information on the nature and the origins of AMDEs. Nevertheless, in order to elucidate the complex mechanisms behind AMDEs different methods should be used in parallel such as radionuclide analysis to locate the origin and transport of air masses.

6 Acknowledgements

Thanks to Kim Holmén for a great visit of Ny-Ålesund and very helpful inputs, interesting lectures. Greetings to the French mercury team, Christophe Ferrari and Olivier Magand, for their inputs, interesting suggestions and a very good time in Tokyo! Financial support from UNIS/NILU is gratefully acknowledged. I am finally very grateful to the Japanese National Institute of Polar Research for helping me participate in the 3rd international symposium on polar research.

7 References

- Arctic Monitoring and Assessment Programme (1998) Assessment report: Arctic pollution Issues. Oslo, AMAP.
- Arctic Monitoring and Assessment Programme (2002) Arctic pollution 2002: Persistent organic pollutants, heavy metals, radioactivity, human health, changing pathways. Oslo, AMAP.
- Banic, C.M., Beauchamp, S.T., Tordon, R.J., Schroeder, W.H., Steffen, A., Anlauf, K.A. and Wong, H.K.T. (2003) Vertical distribution of gaseous elemental mercury in Canada. *J. Geophys. Res.*, 108, doi : 10.1029/2002JD002116
- Beine, H.J., Engardt, M., Jaffe, D.A., Hov, Ø., Holmén, K. and Stordal, F. (1996) Measurements of NO_x and aerosol particles at the NY-Ålesund Zeppelin mountain station on Svalbard: Influence of regional and local pollution sources. *Atmos. Environ.*, 30, 1067-1079.
- Berg, T. and Aspmo, K. (2003) Atmospheric mercury at the Zeppelin station. Kjeller, Norwegian Institute for Air Research (NILU OR 86/2003).
- Berg, T., Sekkeseter, S., Steinnes, E., Valdal, A.-K. and Wibetoe, G. (2003) Springtime depletion of mercury in the European Arctic as observed at Svalbard. *Sci. Tot. Environ.*, 304, 43-51.
- Bergan, T., Gallardo, L. and Rodhe, H. (1999) Mercury in the global troposphere: A three-dimensional model study. *Atmos. Environ.*, 33, 1575-1585.
- Bottenheim, J.W., Galland, A.J. and Brice, K.A. (1986) Measurements of NO_y species and O₃ at 82°N latitude. *Geophys Res. Lett.*, 13, 113-116.
- Dommergue, A., Ferrari, C. and Boutron, C.F. (2003) First investigation of an original device dedicated to the determination of gaseous mercury in interstitial air in snow. *Anal. Bioanal. Chem.*, 375, 106-111.
- Draxler, R.R. and Rolph, G.D. (2003) HYSPLIT (*HYbrid Single-Particle Lagrangian Integrated Trajectory*) Model access via NOAA ARL READY Website (<http://www.arl.noaa.gov/ready/hysplit4.html>). Silver Spring, MD, NOAA Air Resources Laboratory.
- Ebinghaus, R., Koch, H.H., Temme, C., Einax, J.W., Løve, A., Richter, A., Burrows, J.P. and Schroeder, W.H. (2002) Antarctic springtime depletion of atmospheric mercury. *Environ. Sci. Technol.*, 36, 1238-1244.
- Ebinghaus, R., Tripathi, R.M., Wallschlager, D. and Lindberg, S.E. (1999) Natural and anthropogenic mercury sources and their impact on the air-surface exchange of mercury on regional and global scales. In: *Mercury contaminated sites*. Ed. by R. Ebinghaus, R.R. Turner, L.D. de Lacerda, O. Vasiliev. Berlin, Springer. pp. 1-50.

- Gauchard, P.-A., Aspmo, K., Temme, C., Steffen, A., Ferrari, F., Berg, T., Ström, J., Kaleschke, L., Dommergue, A., Bahlmann, E., Magnand, O., Planchon, F., Ebinghaus, R., Banic, C., Nagorski, S., Baussand, P. and Boutron, C. (2005) Study of the origin of atmospheric mercury depletion events recorded in Ny-Ålesund, Svalbard, spring 2003. *Atmos. Environ.*, *39*, 7620-7632.
- Gauchard, P.-A., Ferrari, C.P., Dommergue, A., Poissant, L., Pilote, M., Guehenneux, G., Boutron, C.F. and Baussand, P. (2005) Atmospheric particle evolution during a nighttime atmospheric mercury depletion event in sub-Arctic at Kuujuarapik/Whapmagoostui, Québec, Canada. *Sci. Tot. Environ.*, *336*, 215-224.
- Hansen, J.C. (2000) Environmental contaminants and human health in the Arctic. *Toxicol. Lett.*, *112-113*, 119-125.
- Hollwedel, J., Wenig, M., Beirle, S., Kraus, S., Köhl, S., Wilms-Grabe W., Platt, U. and Wagner, T. (2003) Year-to-year variations of spring time polar tropospheric BrO as seen by GOME. *Advances in Space Research*, *34*, 804-808.
- Imura, N., Sukegawa, E., Pan, S.K., Nagao, K., Kim, J.Y., Kwan, T. and Ukita, T. (1971) Chemical methylation of inorganic mercury with methylcobalamin, a vitamin-B12 analog. *Science*, *172*, 1248-1249.
- Jonasson, I. and Boyle, R. (1972) Geochemistry of mercury and origins of natural contamination of the environment. *Can. Min. Metall. Bull.*, *65*, 32-39.
- Kim, K.-H. and Kim, M.-Y. (2001) A decadal shift in total gaseous mercury concentration levels in Seoul, Korea: changes between the late 1980s and the late 1990s. *Atmos. Environ.*, *36*, 663-675.
- Lindberg, S.E. and Stratton, W.J. (1998) Atmospheric mercury speciation: concentrations and behaviour of reactive gaseous mercury in ambient air. *Environ. Sci. Technol.*, *32*, 49-57.
- Lindberg, S.E., Brooks, S., Lin, C.-J., Scott, K.J., Landis, M.S., Stevens, R.K., Goodsite, M. and Richter, A. (2002) Dynamic oxidation of gaseous mercury in the Arctic troposphere at polar sunrise. *Environ. Sci. Technol.*, *36*, 1245-1256.
- Lindqvist, O. and Rodhe, H. (1985) Atmospheric mercury – a review. *Tellus*, *37B*, 136-159.
- Lu, J.Y., Schroeder, W.H., Barrie, L.A., Steffen, A., Welch, H.E., Martin, K., Lockhart, L., Hunt, R.V., Boila, G. and Richter, A. (2001) Magnification of atmospheric mercury deposition to polar regions in springtime: the link to tropospheric ozone depletion chemistry. *Geophys. Res. Lett.*, *28*, 3219-3222.
- Nriagu, J.O. (1989) A global assessment of natural sources of atmospheric trace metals. *Nature*, *338*, 47-49.

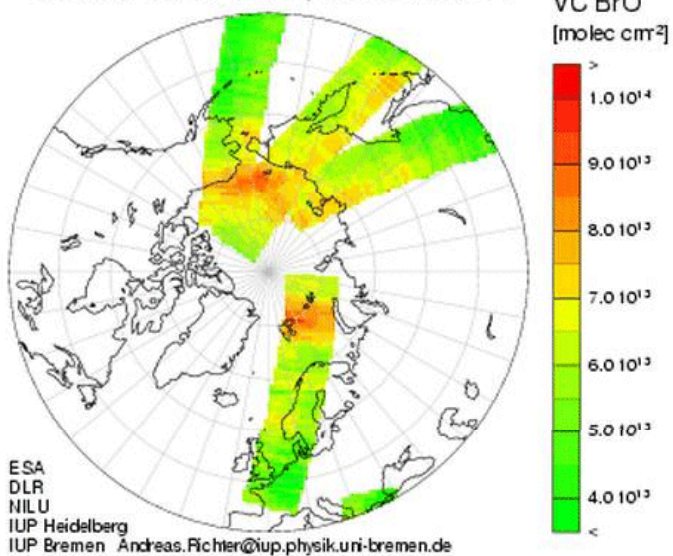
- Pacyna, E.G. and Pacyna, J.M. (2002) Global Emission of Mercury from Anthropogenic Sources in 1995. *Water Air Soil Poll.*, 137, 149-165.
- Poissant, L. (2000) Total gaseous mercury in Québec (Canada) in 1998. *Sci. Tot. Environ.*, 259, 191-201
- Poissant, L., Dommergue, A. and Ferrari, C.P. (2002) Mercury as a global pollutant. *J. Phys. IV*, 12 (PR10), 143-160.
- Rolph, G.D. (2003) Real-time Environmental Applications and Display sYstem (READY) Website (<http://www.arl.noaa.gov/ready/hysplit4.html>). Silver Spring, MD, NOAA Air Resources Laboratory.
- Schmolke, S.R., Schroeder, W.H., Koch, H.H., Schneeberger, D., Munthe, J. and Ebinghaus, R. (1999) Simultaneous measurements of total gaseous mercury at four sites on a 800 km transec: special distribution and short-term variability of total gaseous mercury over central Europe. *Atmos. Environ.*, 33, 1725-1733.
- Schroeder, W. H. and Munthe J. (1998) Atmospheric mercury, an overview. *Atmos. Environ.*, 32, 809-822.
- Schroeder, W.H., Anlauf, K., Barrie, L.A., Lu, J.Y., Steffen, A., Schneeberger, D.R. and Berg, T. (1998) Arctic springtime depletion of mercury. *Nature*, 394, 331-332.
- Skov, H., Christensen, J., Goodsite, M., Heidam, N.Z., Jensen, B., Wählin, P. and Geernaert, G. (2004) Fate of elemental mercury in the Arctic during atmospheric mercury depletion episodes and the load of atmospheric mercury to the Arctic. *Environ. Sci. Technol*, 38, 2373-2382.
- Slemr, F., Schuster, G. and Seiler, W. (1985) Distribution, speciation, and budget of atmospheric mercury. *J. Atmos. Chem.*, 3, 407-434.
- Solberg, S., Schmidbauer, N., Semb, A., Stordal, F. and Hov, Ø. (1996) Boundary-layer ozone depletion as seen in the Norwegian Arctic in spring. *J. Atmos. Chem.*, 23, 301-332.
- Sommar, J., Wängberg, I., Berg, T., Gårfeldt, K., Munthe, J., Richter, A., Urba, A., Wittrock, F. and Schroeder, W.H. (2004) Circumpolar transport and air-surface exchange of atmospheric mercury at Ny-Ålesund (79N), Svalbard, spring 2002. *Atmos. Chem. Phys. Discuss.*, 4, 1727-1771.
- Sprovieri, F., Pirrone, N., Hedgecock, I.M., Landis, M.S. and Stevens, R. (2002) Intensive atmospheric mercury measurements at Terra Nova Bay in Antarctica during November and December 2000. *J. Geophys. Res.*, D107, 4722, doi: 10.1029/2002JD002057.
- Steffen, A., Schroeder, W., MacDonald, R. and Konoplev, A. (2004) On-going atmospheric mercury measurements in the high Arctic in Canada and Russia. *Materials and geo-environment*, 51, 1786-1790.

- Takizava, Y. and Osame, M. (2001) Understanding of Minamata disease Methylmercury poisoning in Minamata and Niigata, Japan. Tokyo, Japan Public Health Association.
- Temme, C., Einax, J., Ebinghaus, R. and Schroeder, W. (2003) Measurements of atmospheric mercury species at a coastal site in the Antarctic and over the South Atlantic Ocean during polar summer. *Environ. Sci. Technol.*, 37, 22-31.
- Watras, C.J., Back, R.C., Halvorsen, S., Hudson, R.J.M., Morrison, K.A. and Wentz, S.P. (1998) Bioaccumulation of mercury in pelagic freshwater food webs. *Sci. Tot. Environ.*, 219, 183-208.

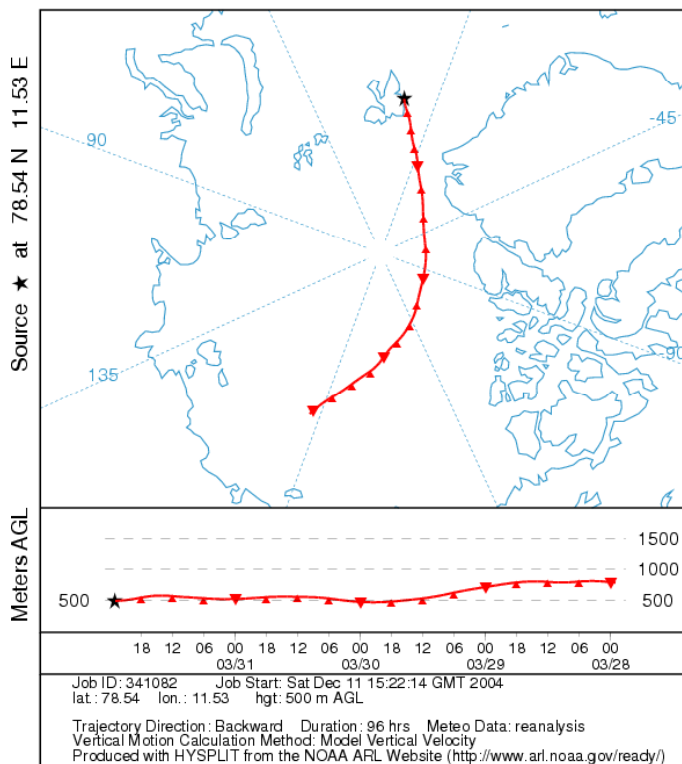
Appendix A

AMDE 1: 31st March / 1st April

GOME NRT BrO, 2003/03/31



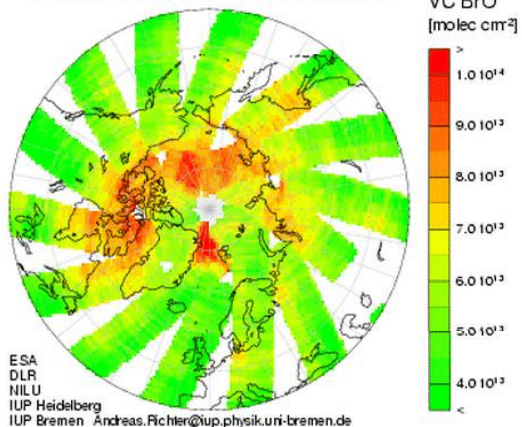
NOAA HYSPLIT MODEL
Backward trajectory ending at 23 UTC 31 Mar 03
CDC1 Meteorological Data



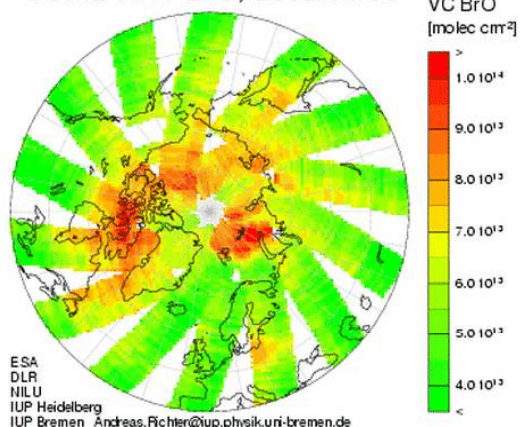
Appendix B

AMDE 2: 8th-10th April

GOME NRT BrO, 2003/04/08

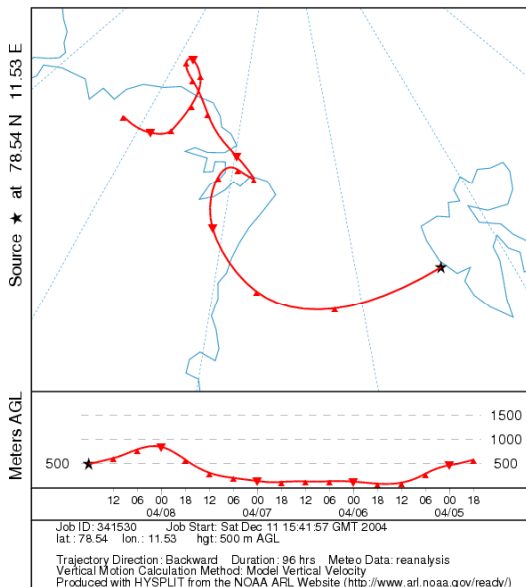


GOME NRT BrO, 2003/04/09



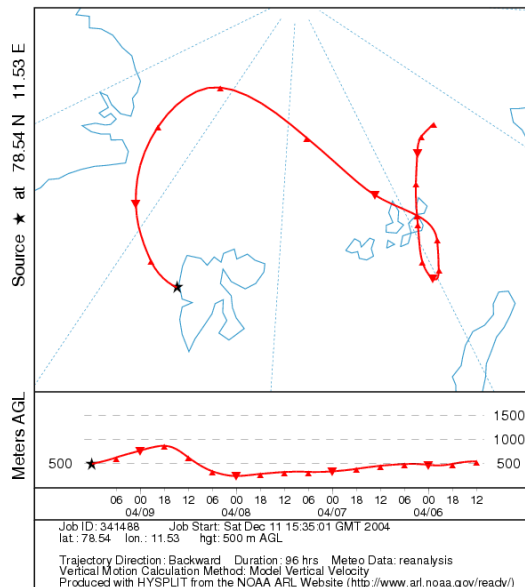
Advection of ADME 2a to Ny-Ålesund

NOAA HYSPLIT MODEL
Backward trajectory ending at 18 UTC 08 Apr 03
CDC1 Meteorological Data



Advection of AMDE 2b to Ny-Ålesund

NOAA HYSPLIT MODEL
Backward trajectory ending at 12 UTC 09 Apr 03
CDC1 Meteorological Data



Appendix C

AMDE 3: 15th-17th May

